04

Damped vacuum discharge as a variant of EUV radiation source for lithography

© L.V. Stepanov, 1,2 P.S. Antsiferov, 1,2 N.D. Matyukhin 1,3

- ¹ Institute of Spectroscopy, Russian Academy of Sciences,
- 108840 Troitsk, Moscow, Russia
- ² National Research University Higher School of Economics,
- 109028 Moscow, Russia
- ³ Moscow Institute of Physics and Technology (National Research University),

141701 Dolgoprudny, Moscow Region, Russia

e-mail: lvstepanov@edu.hse.ru

Received December 17, 2024 Revised February 21, 2025 Accepted February 27, 2025

The paper describes an experimental setup designed to produce a damped vacuum discharge with a peak current of $18 \, \text{kA}$ and a duration of less than $1 \, \mu \text{s}$. In this type of discharge, a previously observed phenomenon is realized —namely, the generation of multicharged ions in a vacuum discharge during the plasma column growing stage, without pinching. The main idea is to rapidly terminate the discharge current immediately after this stage. This may enable the development of a discharge-based radiation source with a low level of electrode erosion. The discharge current is controlled by damping the discharge circuit, achieved by introducing a ballast resistor into the electrical circuit. Test measurements confirmed the formation of multicharged iron ions (up to Fe VIII) at times between 100 and $100-200 \, \text{ns}$ after discharge initiation. The dependence of the discharge development dynamics and the intensity of its emission in the extreme ultraviolet (EUV) range on the electrode gap was studied. EUV emission at a wavelength of 13.5 nm was demonstrated when a tin anode was used in the discharge.

Keywords: electrical discharges, extreme ultraviolet radiation, extreme ultraviolet spectra, multicharged ions.

DOI: 10.61011/TP.2025.07.61449.463-24

Introduction

Due to demand for sources of extreme ultraviolet radiation (EUV $\lambda=8-25\,\mathrm{nm}$) for applications in EUV lithography [1–3], it is interesting to study capabilities of vacuum electric discharges, whose technical implementation is simpler and cheaper than creation of laser plasma. These discharges were studied by means of recorders of EUV radiation based on micro-channel plates (MCP) having time ($\sim 10\,\mathrm{ns}$) and spatial ($\sim 50\,\mu\mathrm{m}$) resolution to detect a number of vacuum discharge properties that are interesting in terms of applications [4,5]. The present paper describes a variant of the EUV radiation source, which is designed based on results of the study [5].

The paper [5] has studied EUV radiation of the vacuum spark plasma of the current of 50 kA (the basic capacitance $3\,\mu\text{F}$, the operating voltage of $12\,\text{kV}$). It was substantial to use a method of simultaneous recording spatial distribution of the plasma and spectrograms of its EUV radiation by means of the MCP detectors (the measurement diagram is shown in Fig. 1). The main result of the study was detection of generation of iron ions Fe VII during plasma discharge column growing at the initial stage of discharge development $(200-300\,\text{ns}$ after discharge current initiation), when the voltage of $12\,\text{kV}$ initially applied to a discharge gap does not have time to drop and is $\sim 5\,\text{kV}$, while the discharge current is of a value of several kiloamperes. At this moment, there

is no plasma pinching. The electron energy (> $100\,\mathrm{eV}$) required to produce the ions Fe VII can be obtained by them as a result of acceleration in a field applied to the plasma (an electron escape phenomenon). This mechanism is possible, if the electric field applied to the plasma is of a value of the critical order (an electron acceleration at the mean free path gives an increase of the kinetic energy of the order of an average thermal energy). The estimates of the paper [5] show that the electric field ($\sim 10^4\,\mathrm{V/cm}$) applied to the discharge plasma will be critical if the electron density does not exceed $\sim 10^{16}\,\mathrm{cm}^{-3}$. These values of the electron

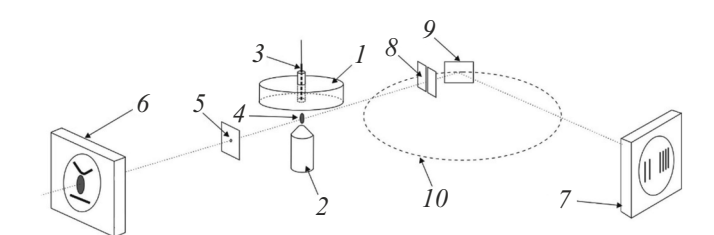


Figure 1. Experimental setup with simultaneous recording of obscuragrams and spectrograms of the discharge: 1—the cathode, 2—the anode, 3—the trigger electrode, 4—the discharge plasma, 5—the pinhole camera, 6—the MCP detector of the pinhole camera, 7—the MCP detector of the spectrometer, 8—the entrance slit of the spectrometer, 9—the diffraction grating of the spectrometer, 10—the Rowland circle.

density are quite realistic at the initial state of discharge formation.

The present study describes the variant of the EUV source based on studying the vacuum discharge plasma, which uses the above-described phenomenon. The main idea is to terminate the discharge current after several hundred nanoseconds after discharge initiation, when radiation of the multicharged ions disappears. At the same time, substantial decrease of total erosion of electrodes is expected in comparison with a discharge circuit described in the paper [5]. This erosion causes contamination of optical elements, which is one of the main drawbacks of the discharge-based EUV radiation sources. The simplest method of creation of this discharge is to introduce damping into the discharge circuit. Description of the electric circuit of this discharge is given below with results of test measurements.

1. Description of the discharge circuit

The complete electric diagram of the discharge circuit is shown in Fig. 2. The main discharge circuit includes low-inductance capacitor KPIM-50-0.15 (the electric capacitance $C_0=0.15\,\mu\text{F}$, the inductance $L=10\,\text{nH}$). This capacitance is significantly lower than that used in the paper [5] $(3\,\mu\text{F})$. The operating voltage in the present experiments was $U_0=12\,\text{kV}$. The complete design inductance L_0 that is measured by a period of current oscillations $(T=1.7\,\mu\text{s})$ was $L_0=91\,\text{nH}$. The near-critical damping (that ensures effective termination of the discharge current) is achieved by introducing the active resistance $R_4=0.7\,\Omega$ into the discharge circuit. The nominal values of the resistors of Fig. 2: $R_1=800\,\Omega$, $R_2=300\,\text{k}\Omega$, $R_3=15\,\text{k}\Omega$. The resistance R_4 is assembled from 30 parallel resistors TVO-05 of the nominal value of $22\,\Omega$.

The discharge is initiated by the trigger electrode 4 (Fig. 2), which is energized with a pulse of negative-polarity

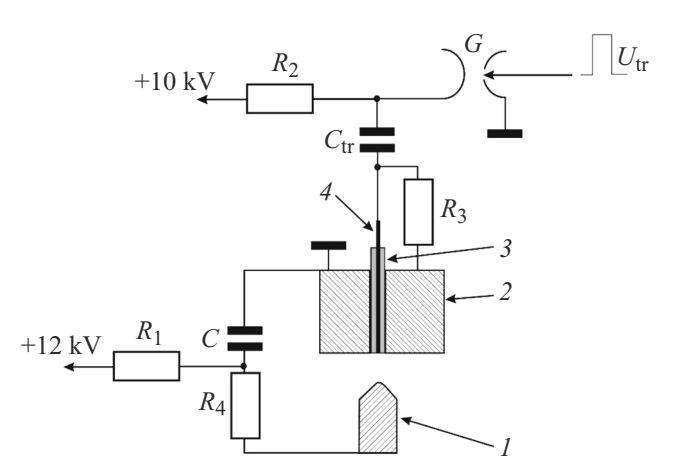


Figure 2. Electric diagram of the discharge circuit: I — the anode, 2 — the cathode, 3 — the insulator of the trigger electrode, 4 — the trigger electrode, G — the discharger of the trigger circuit RU-62.

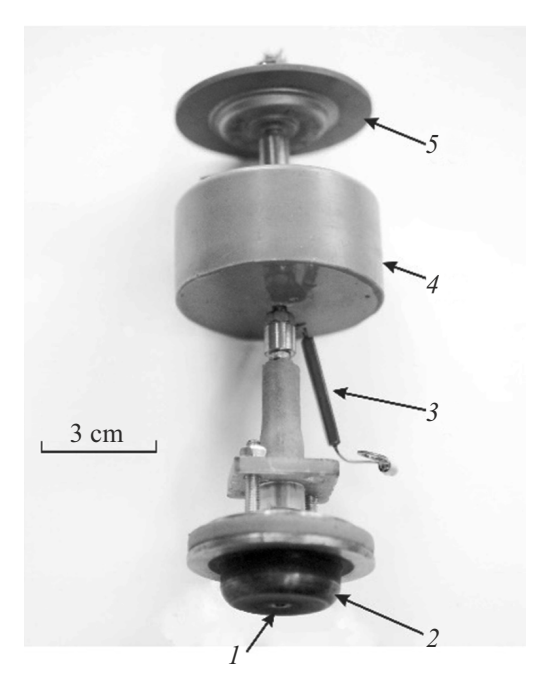


Figure 3. Design of the cathode assembly: I — the hole of the trigger electrode, 2 — the cathode, 3 — the grounding resistor R_3 , 4 — the capacitor K15-4, 5 — the discharger RU-62.

voltage of $-10\,\mathrm{kV}$. The trigger discharge circuit consists of the capacitor K15-4 with the capacitance $C_{\mathrm{tr}}=4.7\,\mathrm{nF}$ and the discharger RU-62. In order to reduce inductance of a discharge ignition circuit, the capacitor, the trigger discharger G and the cathode were assembled as a single unit without connecting cables (in the study [5], a trigger pulse was applied to the electrode 4 through a cable section of resistance of $50\,\Omega$ and the length of $1.5\,\mathrm{m}$). Fig. 3 shows the cathode unit with a removed coaxial return current conductor. This design makes it possible tor increase a rate of arrival of the trigger plasma at the initial discharge stage with substantial decrease of the energy in the trigger circuit and reduction of a level of erosion of the cathode electrode (in the paper [5] the value of C_{tr} was $50\,\mathrm{nF}$)

The anode electrode had a diameter of 3 mm, and during the experiment the anode—cathode distance varied from 1 to 5 mm. An apex angle of the anode electrode cone is 90° , the rounding radius is 0.2 mm. The electrodes are made of iron. The residual pressure in the discharge chamber is 10^{-2} Pa. The discharge current was measured by means of a magnetic probe. Fig. 4 shows the discharge current curve without the damping resistance of the study [5] (the curve I) and the current discharge curve with the damping resistance (the curve I). In case of damping, the main part of the energy stored in the capacitor is released in a ballast resistor I0, rather than in the discharge, which shall result in reduction of the level of electrode erosion. The time of the graph of Fig. 4 was counted from the moment of initiation of the trigger electrode current.

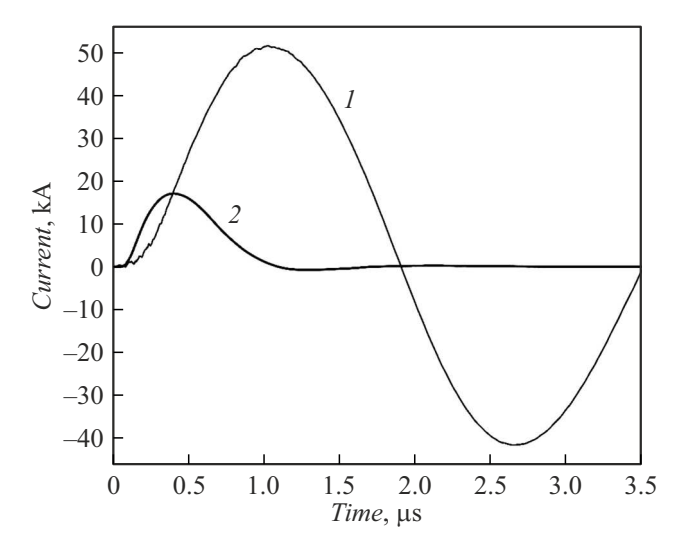


Figure 4. Discharge current: I — the discharge current curve without the damping resistance [5], 2 — the curve of the damped-discharge current (the present study).

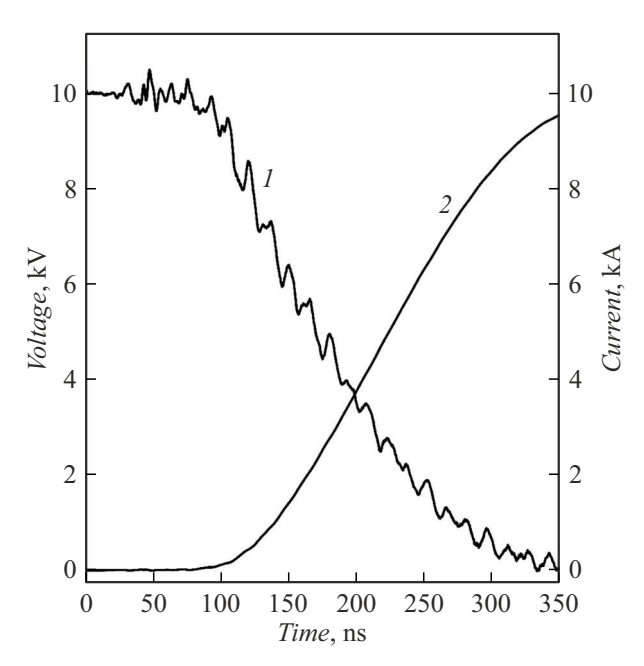


Figure 5. Time dependence of the voltage (I) at the discharge gap and the current (2) therethrough at the initial discharge stage.

As shown in the paper [5], origination of EUV radiation at the initial discharge stage is related to a relatively slow voltage drop at the discharge gap. In the present study, information about this voltage was indirectly obtained by numerically solving the Kirchhoff equation for the main discharge circuit:

$$U(t) = U_0 - \frac{1}{C} \int_0^t dI(t)dt - R_4 I(t) - L_0 \frac{dI(t)}{dt}.$$
 (1)

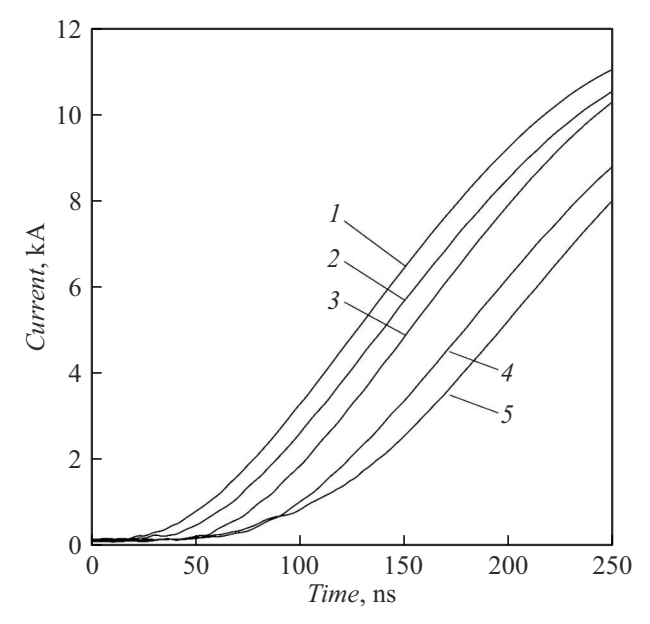


Figure 6. Discharge current curves at the initial stage of development with various distances between the anode and the cathode, [mm]: I - 1, 2 - 2, 3 - 3, 4 - 4, 5 - 5.

The values of the magnitudes in the equation are given at the beginning of the chapter, the integral and the derivative of the current were numerically taken by an experimental curve. The obtained time dependence of the voltage at the discharge gap with its respective current curve is shown on Fig. 5. As can be seen, the voltage drops not instantly, and within the interval from 100 to 200 ns after discharge initiation the voltage 4–8 kV is applied to the discharge gap, while at the same time the current 2–4 kA is flowing therethrough. Thus, damping made it possible to limit the discharge in time, with keeping key features of its initial stage.

The discharge current curves were recorded to show a dependence of delay of a moment of origination of the discharge current in relation to the trigger pulse on the distance between the electrodes (Fig. 6). Increase of the delay with the large anode—cathode distances is related to increase of the time of filling the discharge gap with the plasma that results in its short circuiting. The respective change of EUV radiation dynamics is described below.

2. Test measurements

Due to changes in a design of the discharge circuit in comparison with a design of an installation provided in [5], it was important in the present study to check availability of the stage of origination of multicharged iron ions at the initial discharge stage. For this purpose, there was a number of measurements, which simultaneously in a single discharge recorded an EUV spectrum and a spatial structure of the plasma with time resolution (see Fig. 1 for a measurement diagram).

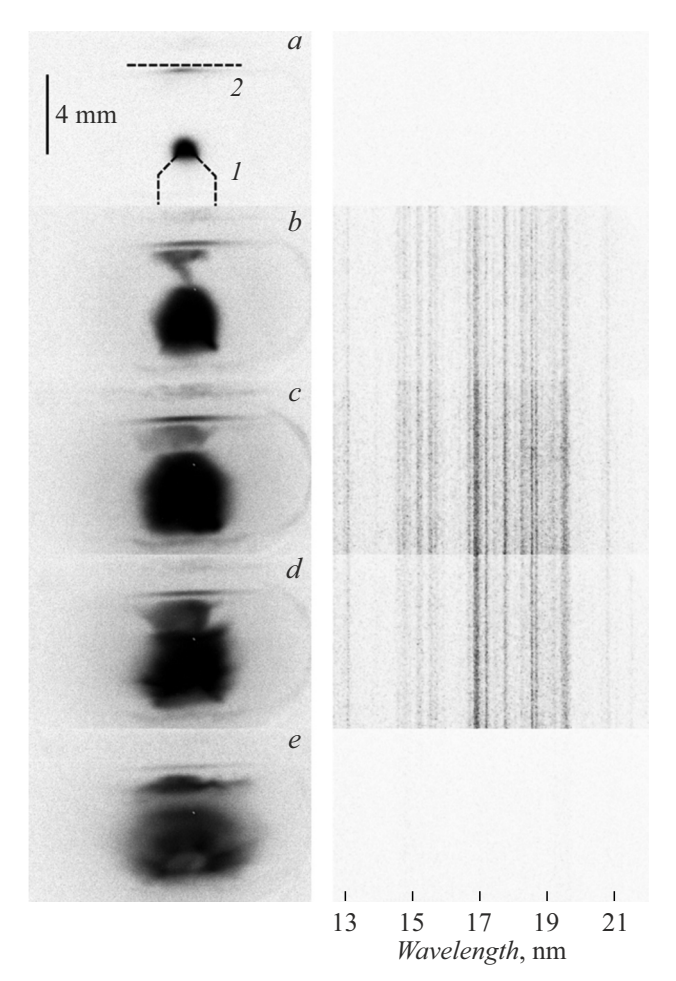


Figure 7. Dynamics of discharge development and the respective spectrograms. The delay in relation of the trigger pulse, [ns]: a-60, b-100, c-130, d-150, e-190. a- positions of the electrodes are presented: I- the anode, 2- the cathode. The image is given in a negative.

A spectrum composition of discharge radiation was studied in this paper by using a glazing incidence spectrometer with a shifted slit [6]. It is specifically designed to obtain focusing of the spectrum perpendicular to a line of sight, which in turn makes it possible to use detectors based on the micro-channel plates for recording the spectrum. In order to achieve this effect, the spectrum slit is shifted inside the Rowland circle, while a recording plane is moved outwardly. The geometrical parameters of the spectrometer: the lattice radius is $R = 1 \,\mathrm{m}$, the groove density is 600 grooves/mm, the grazing angle is 6° , the distance from the entrance slit to the grating 53 mm, the distance from the grating to the recording plane is 420 mm (Fig.1). The parameters were selected in accordance with calculations of the paper [6]. The spatial structure of the plasma was recorded by means of the pinhole camera with the hole diameter of 0.1 mm and geometrical magnification of 3. The recorders based on the micro-channel plates with an exposure time of 20 ns were used as an image recording system. They are activated simultaneously by a strobing pulse, whose generator is

synchronized with the discharge trigger pulse. It was possible to smoothly adjust a delay of the strobing pulse in relation to the time of discharge initiation. A more detailed description of the measurement diagram is given in the paper [5].

Fig. 7 shows a number of obscuragrams and spectrograms that correspond thereto for the various times in the case of the anode-cathode distance of 4 mm. The initial phase of filling the discharge gap with the plasma exhibits anode evaporation under impact of an electron beam, which originates due to application of the high voltage thereto (Fig. 7, a). At this stage, the discharge current is small (Fig. 5, the delays 0-50 ns). This phenomenon was already noticed in the first studies of a low-inductance vacuum spark [7]. At this moment, there is no radiation of the multicharged ions. Then, it appears in the delay range 70-150 ns (Fig. 7, b-d) and disappears after the 200-th nanosecond (Fig. 7, e). Fig. 8 shows a digitized spectrogram that corresponds to Fig. 7, c. The lines are identified in accordance with the NIST database [8], the spectrum has lines of the ions Fe VII and Fe VIII recorded.

The dynamics of EUV radiation depending on the anode-cathode distance was also studied. Fig. 9 shows a dependence of spectrum-integral intensity on time for various values of the distance between the anode and the cathode. Each histogram column corresponds to a separate spectrum with a respective time delay. The present time dependence of average intensity of EUV radiation shall be understood as a smooth curve that approximates a column height. At the distance of 1 mm, the spectrum intensity is very small (Fig. 9, a). With increase of the distance to 2 mm, glowing occurs in about 75 ns after the trigger pulse and continues throughout a rise of current in the discharge (Fig. 9, b). With further increase of the distance between the electrodes, the glowing gets more intense, while its duration is reduced to approximately 50 ns (Fig. 9, c). At the distances of 3, 4 and 5 mm between the anode and the cathode, a nature of the radiation dynamics remains the same, whereas with increase of the distance a moment of maximum radiation intensity is shifted from 100 to 150 ns after discharge initiation (Fig. 9, c-e).

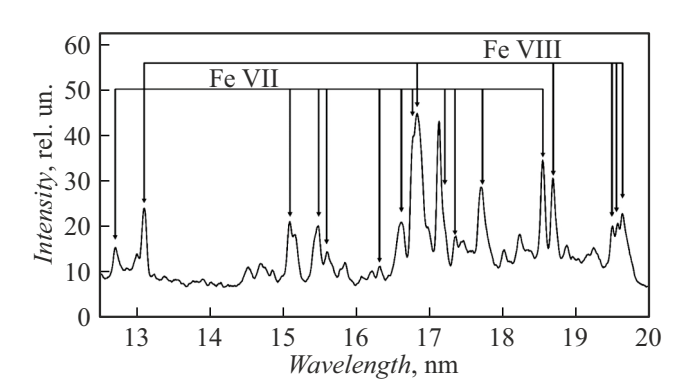


Figure 8. Spectrum that corresponds to Fig. 7, c (130 ns). The positions of the lines Fe VII and Fe VIII are specified in accordance with a database. NIST [8].

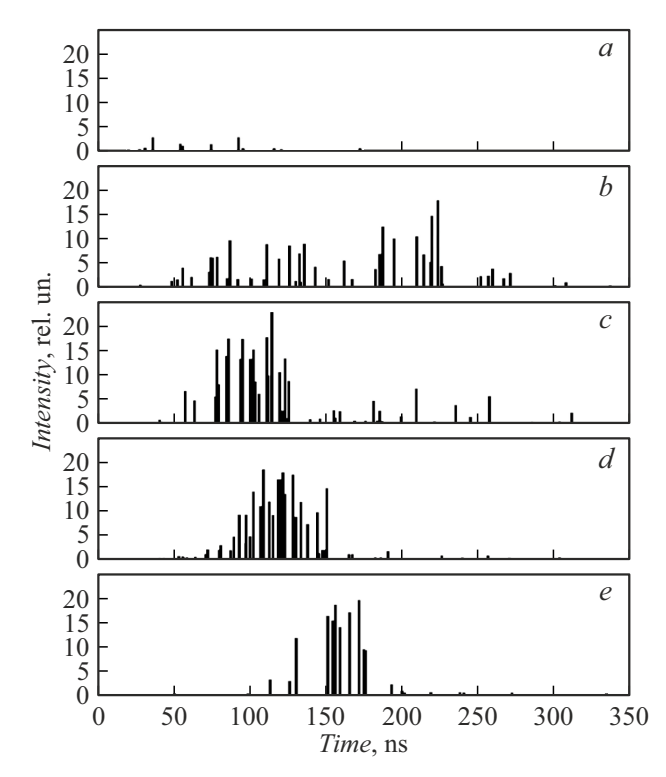


Figure 9. Dependence of source radiation intensity on time for the various distances between the electrodes. The distance between the anode and the cathode, [mm]: a-1, b-2, c-3, d-4, e-5.

3. Discussion

The initial phase of discharge development, which was found in the study [5] and characterized by glowing of the multicharged ions, was reproduced in a damped-circuit discharge. Unlike the previous implementation, when the glowing originated after the 200-th nanosecond to hold approximately until the 300-th nanosecond, in the present study the glowing appeared already in 100 ns after discharge initiation. It is supposed that it may be related to decrease of inductance of the trigger discharge circuit, which provided fast shooting-in of matter into the discharge gap. Implementation of a frequency mode of operation of the discharge circuit requires application of a system for cooling the ballast resistor R_4 .

Detailed analysis of physical phenomena in the discharge is not included in the present study. An upper estimate of the electron density, which is given in the paper [5] $(n_e < 10^{16} \, {\rm cm}^{-3})$, shows that the discharge plasma has a density that is relatively small for high-current discharges. It is incorrect to talk about an electron temperature in conditions of electron acceleration in the field applied to the plasma, and it follows from a fact of observation of the multicharged iron ions that the average electron energy shall be about hundreds of eV.

The research included the test measurements with the tin anode. All the electric discharge parameters corresponded

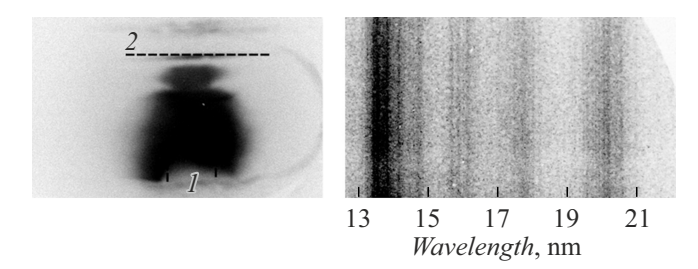


Figure 10. Obscuragram and respective spectrogram of the tinanode discharge. The time after discharge initiation is 120 ns. The images is given in a negative: I—the anode, 2—the cathode.

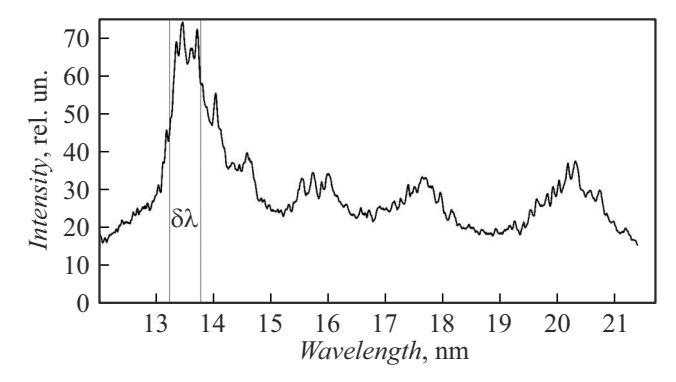


Figure 11. Spectrum that corresponds to Fig. 10. $\delta\lambda$ is a range used in EUV lithography [9].

to experiments with an iron anode. The dynamics of development of the discharge current has not undergone any noticeable change after replacement of the anode material. The anode—cathode distance was 4 mm. The obscuragram and the spectrogram of the tin-anode discharge are shown in Fig. 10 and the respective digitized EUV spectrogram is given in Fig. 11. Its radiation spectrum exhibits an intense group of lines around 13.5 nm, which is used in an EUV lithography technology. Fig. 11 specifies a reflection range of the Mo—Si-multilayer mirror that is applied in technological optical circuits [9]. Evaluation of prospects of realistic practical applications of the described discharge variant requires a study of efficiency of energy transformation and optimization of the discharge parameters as well.

Conclusion

We present the damped vacuum discharge that is a source of EUV radiation of the multicharged iron ions without pinching with the potentially low level of electrode erosion. It includes parameters of the electric circuit, which make it possible to achieve a critical mode in the oscillation discharge circuit. The dependence of the discharge dynamics on the distance between the electrodes has been studied. The optimal distance for achieving the maximum intensity of EUV radiation was 3–5 mm. It is

found that radiation of the damped discharge at the earlier stage of development as well as radiation of the undamped discharge [5] has the lines of the multicharged ions Fe VII and Fe VIII. It is demonstrated that it is possible to obtain radiation of the multicharged tin ions with the wavelength of 13.5 nm, which can make the proposed discharge variant relevant for applications in EUV lithography. Future plans of research that is related to the presented discharge type include modeling of physical processes and optimization of the discharge parameters as a radiation source.

Funding

This study was carried out under State assignment FFUU-2025-0005.

Conflict of interest

The authors declare that they have no conflict of interest.

References

- J. Beckers, T. van de Ven, R. van der Horst, D. Astakhov, V. Banine. Appl. Sci., 9, 2827 (2019).
 DOI: 10.3390/app9142827
- [2] D.B. Abramenko, P.S. Antsiferov, D.I. Astakhov, A.Yu. Vinokhodov, I.Yu. Vichev, R.R. Gayazov, A.S. Grushin, L.A. Dorokhin, V.V. Ivanov, D.A. Kim, K.N. Koshelev, P.V. Krainov, M.S. Krivokorytov, V.M. Krivtsun, B.V. Lakatosh, A.A. Lash, V.V. Medvedev, A.N. Ryabtsev, Yu.V. Sidelnikov, E.P. Snegirev, A.D. Solomyannaya, M.V. Spiridonov, I.P. Tsygvintsev, O.F. Yakushev, A.A. Yakushkin. UFN, 189, 323 (2019) (in Russian). DOI: 10.3367/UFNr.2018.06.038447
- [3] V.Y. Banine, K.N. Koshelev, G.H.P.M. Swinkels. J. Phys. D: Appl. Phys., 44, 253001 (2011).
 DOI: 10.1088/0022-3727/44/25/253001
- [4] P.S. Antsiferov, L.A. Dorokhin. Fizika plazmy, 48 (in Russian).(11), 1086 (2022). DOI: 10.31857/S0367292122600492
- P.S. Antsiferov, L.V. Stepanov, N.D. Matyukhin. Fizika plazmy, (in Russian). 50 (6), 701 (2024).
 DOI: 10.31857/S0367292124060076
- [6] P.S. Antsiferov, L.A. Dorokhin, P.V. Krainov. Rev. Sci. Instrum., 87 (5), 053106 (2016). DOI: 10.1063/1.4945654
- [7] T.N. Lie, R.C. Elton. Phys. Rev. A, 3, 865 (1971).DOI: 10.1103/PhysRevA.3.865
- [8] A. Kramida, Yu. Ralchenko, J. Reader. and NIST ASD Team (2023). NIST Atomic Spectra Database (version 5.11), [Online]. Available: https://physics.nist.gov/asd [Mon Aug. 26, 2025]. National Institute of Standards and Technology, Gaithersburg, MD
- [9] I. Fomenkov, D. Brandt, A. Ershov, A. Schafgans, Y. Tao, G. Vaschenko, S. Rokitski, M. Kats, M. Vargas, M. Purvis, R. Rafac, B. La Fontaine, S. De Dea, A. LaForge, J. Stewart, S. Chang, M. Graham, D. Riggs, T. Taylor, M. Abraham, D. Brown. Adv. Opt. Technol., 6,173 (2017).
 DOI: 10.1515/aot-2017-0029

Translated by M.Shevelev